Available online at www.sciencedirect.com
ScienceDirect
Journal of Solid State Chemistry 179 (2006) 3052–3058
JOURNAL OF SOLID STATE CHEMISTRY
www.elsevier.com/locate/jssc

Magnetic susceptibility, specific heat and magnetic structure of $CuNi_2(PO_4)_2$

Jaione Escobal[a], José L. Pizarro[b], José L. Mesa[a,*], Aitor Larrañaga[b], Jesús Rodríguez Fernández[c], María I. Arriortua[b], Teófilo Rojo[a]

[a]*Departamento de Química Inorgánica, Facultad de Ciencia y Tecnología, Universidad del País Vasco, EHU. Apdo. 644, E-48080 Bilbao, Spain*
[b]*Departamento de Mineralogía y Petrología, Facultad de Ciencia y Tecnología, Universidad del País Vasco, EHU. Apdo. 644, E-48080 Bilbao, Spain*
[c]*CITIMAC, Facultad de Ciencias, Universidad de Cantabria, Avenida de los Castros, 39005 Santander, Spain*

Received 1 March 2006; received in revised form 10 May 2006; accepted 28 May 2006
Available online 3 June 2006

Abstract

The $CuNi_2(PO_4)_2$ phosphate has been synthesized by the ceramic method at 800 °C in air. The crystal structure consists of a three-dimensional skeleton constructed from MO_4 (M^{II} = Cu and Ni) planar squares and M_2O_8 dimers with square pyramidal geometry, which are interconnected by $(PO_4)^{3-}$ oxoanions with tetrahedral geometry. The magnetic behavior has been studied on powdered sample by using susceptibility, specific heat and neutron diffraction data. The bimetallic copper(II)–nickel(II) orthophosphate exhibits a three-dimensional magnetic ordering at, approximately, 29.8 K. However, its complex crystal structure hampers any parametrization of the *J*-exchange parameter. The specific heat measurements exhibit a three-dimensional magnetic ordering (λ-type) peak at 29.5 K. The magnetic structure of this phosphate shows ferromagnetic interactions inside the Ni_2O_8 dimers, whereas the sublattice of Cu(II) ions presents antiferromagnetic couplings along the *y*-axis. The change of the sign in the magnetic unit-cell, due to the [1/2, 0, 1/2] propagation vector determines a purely antiferromagnetic structure.

Keywords: Mixed Copper(II)–Nickel(II) phosphate; Susceptibility; Specific heat; Magnetic structure

1. Introduction

The study of phosphates of transition elements with low oxidation states has received great interest in recent years. The great ability of phosphate frameworks to stabilize different oxidation states is produced for the relatively high charge in $(PO_4)^{3-}$ tetrahedral that favors the formation of anionic frameworks with a high degree of mechanical, chemical, and thermal stability [1,2]. These compounds offer a considerable number of structures which can give rise to original physical properties (magnetic, heterogeneous catalysis, ion exchange, optical, etc.) with potential applications. Many of the studies in these systems have been carried out on mineral samples. Nevertheless, the ceramic method can be used in the syntheses of these phases giving rise to new compounds with interesting structural characteristic and physical properties. Suitable single-crystals for X-ray structural determination are difficult to obtain by this preparative chemical method, so, the most part of the compound are obtained as powdered samples which are characterized by X-ray powder diffraction techniques, and then studied their magnetic properties by using the SQUID magnetometer and the neutron diffraction methods.

A large number of distinct structural types for compounds represented as $M_3P_2O_8$ are known. Amongst these only the sarcopside $Fe_3(PO_4)_2$ structure [3] is based upon a close-packed array of oxygen atoms. In fact this structure is olivine-like [4] with vacant cation site ordered and results in a change from an orthorhombic to a monoclinic cell. Joubert et al. [5] have shown that a metastable sarcopside-like structure can be formed by the reaction of olivinite-like $Li_2M_2P_2O_8$ plus MSO_4, with M = Mg or Co at reaction temperatures of 933 and 953 K, respectively. The crystal structure of the $Ni_3(PO_4)_2$ phase is isotypic with that of

*Corresponding author. Fax: +34 946013500.
E-mail address: joseluis.mesa@ehu.es (J.L. Mesa).

0022-4596/$ - see front matter © 2006 Elsevier Inc. All rights reserved.
doi:10.1016/j.jssc.2006.05.034

sarcopside, which is related to that of olivine with vacant cation sites ordered [6]. This compound crystallizes in the monoclinic $P2_1/c$ space group. The compound exhibits a three-dimensional crystal structure constructed from trimeric $Ni(2)O_6$–$Ni(1)O_6$–$Ni(2)O_6$ edge-sharing octahedra interconnected through the $(PO_4)^{3-}$ oxoanions. The crystal structure of $CuNi_2(PO_4)_2$ shows a relationship with that corresponding to the $Cu_3(PO_4)_2$ compound [7], which crystallizes in the P-1 triclinic system. In the $Cu_3(PO_4)_2$ phase, the Cu(II) ions occupy two independent positions in the crystal structure. One of them Cu(I) is on a symmetry center. On this site the Cu(II) ions is surrounded by four oxygen forming a slightly distorted planar square geometry. The other site, Cu(2), is in a general position inside a distorted square–planar pyramid, forming a dimer of the Cu_2O_8 type. The main diffences in the topology of the $Cu_3(PO_4)_2$ and $CuNi_2(PO_4)_2$ phases are due to the relative orientations between the dimeric entities. This way, in the $CuNi_2(PO_4)_2$ phase the Ni_2O_8 dimers are rotated approximately 90° from each other along the crystallographic [110] directions, whereas in the $Cu_3(PO_4)_2$ phase the Cu_2O_8 dimers are aligned along the [011] direction from its triclinic cell [7]. The $CuNi_2(PO_4)_2$ phase with a ratio Ni/Cu of 2:1 has adopted a structure related to the anhydrous copper phosphate and not corresponding to the anhydrous nickel posphate, forcing the Ni(II) ions to be located in an unusual five-fold coordination.

Recently, the magnetic behavior and the magnetic structure of $Ni_3(PO_4)_2$ which exhibits antiferromagnetic couplings with a Neel temperature of 17.1 K has been reported. The magnetic structure of this phase is consistent with an antiferromagnetic behavior with the presence of ferromagnetic couplings inside the $Ni(2)O_6$–$Ni(1)O_6$–$Ni(2)O_6$ edge-sharing trimer units [8]. Forsyth et al. resolved the magnetic structure of triclinic $Cu_3(PO_4)_2$ that has a Neel temperature of 22.5 K. This phase exhibits an antiferromagnetic collinear structure with equal magnetic moments on each of the two crystallographic inequivalent Cu(II) ions [9].

In this work and as a part of our research in the field of phosphate and arsenate compounds [10–16] we, here, report on the magnetic, specific-heat measurements together with the magnetic structure of a new bimetallic orthophosphate, with the $CuNi_2(PO_4)_2$ formula.

2. Experimental

The $CuNi_2(PO_4)_2$ phase was synthesized by solid-state reaction in air starting from $Cu(NO_3)_2 \cdot 3H_2O$, $Ni(NO_3)_2 \cdot 6H_2O$ and $(NH_4)(H_2PO_4)$. Stoichiometric quantities of these materials were ground together in an agate mortar. The resulting mixture was heated in an open crucible at 300 °C to decompose all initial reactants. This process was followed by further heating at 800 °C for 20 h with an intermediate regrinding after 10 h. The final product was quenched to room temperature. The obtained compound was cleaned with water and dried over P_2O_5 for 24 h. The contents of Cu, Ni and P in the microcrystalline powdered sample was confirmed by inductively coupled plasma atomic emission spectroscopy (ICP-AES). This synthetic procedure is different from that used by Goñi et al. [15] in order to obtain this phase by calcination at 800 °C during 3 h from the $Cu_{0.9}Ni_2(PO_4)_{1.9}$ $(HPO_4)_{0.02} \cdot 4H_2O \cdot 1.5CH_3OH$.

X-ray powder diffraction pattern was collected on a PHILIPS X'PERT automatic diffractometer operating at 40 kV and 40 mA. Cu–$K\alpha$ radiation ($\lambda = 1.5418$ Å) was employed with steps of 0.02° in 2θ and a fixed counting time of 5 s. The X-ray powder diffraction data were used to evaluate the purity of the product obtained in the synthesis. The data were fitted with the Rietveld method using the FULLPROF program [17,18]. For the $CuNi_2(PO_4)_2$ phosphate the monoclinic unit cell, the $P2_1/n$ space group, and the fractional coordinates previously determined from X-ray powder diffraction data by Goñi et al. [15] were used. The X-ray refined lattice parameters are $a = 6.394(1)$, $b = 9.301(1)$, $c = 4.729(1)$ Å, $\beta = 90.68(1)°$. The reported parameters in Ref. [15] are $a = 6.393(1)$, $b = 9.325(1)$, $c = 4.718(1)$ Å, $\beta = 90.71(1)°$.

Neutron powder diffraction patterns were collected at room temperature on the high resolution D2B powder diffractometer ($\lambda = 1.594$ Å) at the Institut Laue-Langevin in Grenoble. About 5 g of $CuNi_2(PO_4)_2$ were employed in the experiments, placed in a cylindrical vanadium container and held in a liquid helium cryostat. Extensive and accurate diffraction data at 100 and at 2.0 K were recordered over a large angular range $0 \leqslant 2\theta \leqslant 160°$. The data were fitted using the FULLPROF program [18]. The diffractograms were fitted with a six polynomial background using the pseudo-Voigt function to generate the line shape of the diffraction peaks. The refined lattice parameters were $a = 6.3848(2)$, $b = 9.2925(2)$, $c = 4.727(1)$ Å, $\beta = 90.659(2)°$ for 100 K and $a = 6.383(1)$, $b = 9.293(1)$, $c = 4.721(1)$ Å, $\beta = 90.68(1)°$ for 2.0 K.

Magnetic susceptibility measurements were performed on polycrystalline sample between 1.8 and 300 K, using a Quantum Design MPSM-7 magnetometer with a magnetic field of 0.1 T, at which the magnetization vs. magnetic field is linear, even at 5.0 K. Heat capacity measurements were carried out between 1.8 and 300 K by a relaxation method with a PPMS system and using a two tau model analysis. The sample was a plate of 0.25 mm thickness and 4 mg weight obtained by compressing the original powder.

3. Results and discussion

3.1. Magnetic behavior

The magnetic measurements of the $CuNi_2(PO_4)_2$ compound were recordered from room temperature down to 1.8 K and are shown in Fig. 1. A maximum in the molar magnetic susceptibility is observed at 29.8 K indicating the existence of 3D antiferromagnetic interactions in good agreement with the structural data. The thermal evolution

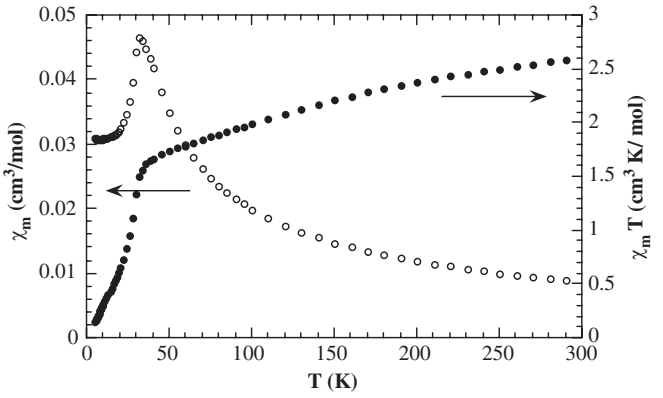

Fig. 1. Thermal evolution of the χ_m and $\chi_m T$ versus T curves of $CuNi_2(PO_4)_2$.

of the molar magnetic susceptibility follows a Curie–Weiss law above 150 K (see Fig. 2), in opposition with that observed by Goñi el al. for the $CuNi_2(PO_4)_2$ compound obtained by calcination of $Cu_{0.9}Ni_2(PO_4)_{1.9}(HPO_4)_{0.02}\cdot 4H_2O\cdot 1.5CH_3OH$ [15], which does not follow the Curie–Weiss law in the entire range of temperatures measured. The values of the Curie and Curie–Weiss constants for the title compound are $3.18\,cm^3\,K/mol$ and $\theta = -66.8\,K$, respectively. This Weiss constant is lower than that obtained for $Ni_3(PO_4)_2$ ($4.08\,cm^3\,K/mol$) [8], in good agreement with the minor amount of Ni(II) cation for the first phase. In fact, if we assume that the $\mu_{eff.}$ for the Ni(II) ions in $CuNi_2(PO_4)_2$ is similar to that in the $Ni_3(PO_4)_2$ phase (3.29 BM), we obtain for the Cu(II) cation an effective paramagnetic moment of 1.92 BM. The $\chi_m T$ vs. T curve for the title compound decreases from $2.6\,cm^3\,K/$ mole at room temperature to $0.002\,cm^3\,K/mole$ at 1.8 K, showing an inflexion point at approximately 35 K after which the curve decreases dramatically. These results are in good agreement with the existence of antiferromagnetic interactions.

3.2. Specific heat measurements

The specific heat data collected between 1.8 and 100 K are shown in Fig. 3. The C_p curve shows a peak (λ-type) at, approximately, 29.5 K, that indicates the establishement of a magnetic ordering at this temperature. Above the magnetic transition, the continuous increase of specific heat with increasing temperature is due to the lattice contribution ($C_{p_{pho}}$). The experimental data do not show saturation up to room temperature. This causes that at 300 K the C_p value is 213 kJ/mol, smaller than the expected 324.2 kJ/mol, considering the Dulong and Petit law [19]. In order to estimate $C_{p_{pho}}$, the specific heat data have been fitted to the Debye model [20]. In this compound, the simplest model, which is able to fit the experimental data, is to consider the existence of two different phonon spectra. This way, if the number of atoms in the unit-cell is N, we suppose n_1 atoms with a Debye temperature θ_1; and $n_2 = 13-n_1$ atoms with a Debye temperature θ_2, the total

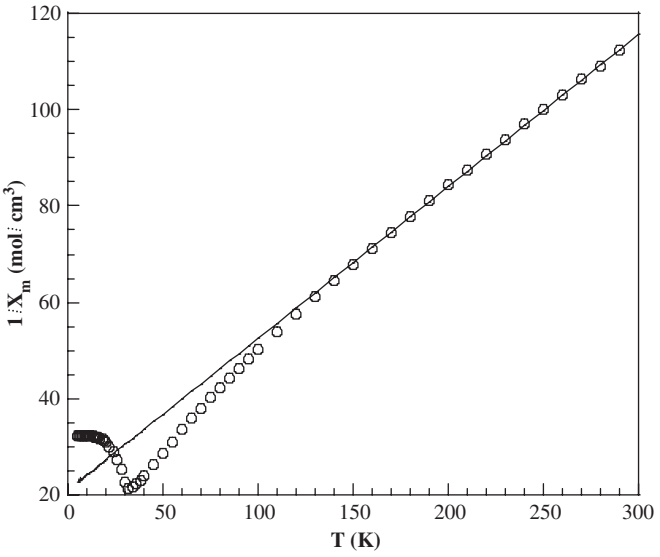

Fig. 2. Thermal evolution of the $1/\chi_m$ versus T curve of $CuNi_2(PO_4)_2$.

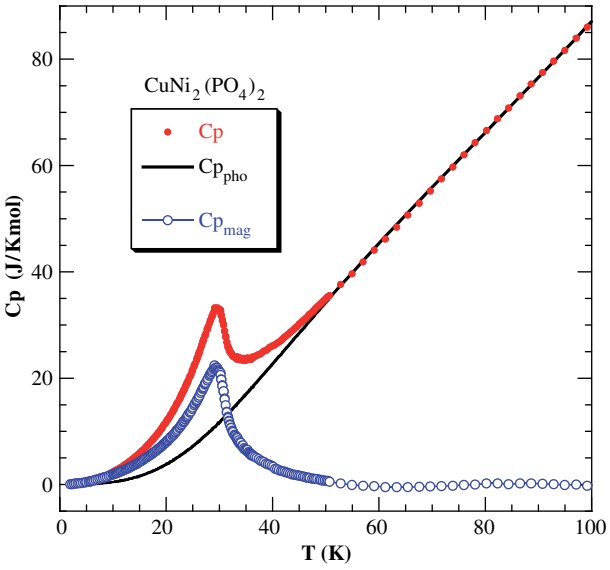

Fig. 3. Specific-heat (C_p) of $CuNi_2(PO_4)_2$. $C_{P_{pho}}$ and $C_{P_{mag}}$ are the estimated phonon and magnetic contributions, respectively.

number of atoms in the chemical formula of the compound being 13. So, in Eq (1) there are three free parameters.

$$C_{p_{Pho}}(T) = n_1 C_{p_{Pho}}(\theta_{D1}) + (13-n_2) C_{p_{Pho}}(\theta_{D2}), \quad (1)$$

where, $C_{pho}(\theta_D) = 9R\left(\frac{T}{\theta_D}\right)^3 \int_0^{\theta_D/T} \frac{x^4 e^x\,dx}{(e^x-1)^2}$.

The best fit well above the temperature of the λ-type peak, shown in Fig. 3 as a solid line, is obtained from $n_1 = 3$, $\theta_{D1} = 235\,K$ and $\theta_{D2} = 850\,K$. The good quality of the fit allows us to consider that this phenomenological model determines quite well the phonon contribution. In addition, the obtained parameters are reasonable: $n_1 = 3$ correspond to the number of the heaviest atoms (Cu and Ni) which have associated a Debye temperature lower than

the room one, whereas, $n_2 = 9$ correspond to the lighter atoms with a higher Debye temperature. These Debye temperatures are similar to those found in other phosphate compounds [21].

The magnetic contribution was calculated as $C_{p_{mag}} = Cp - C_{p_{pho}}$ (see Fig. 3). In this figure a clear maximum at 29.5 K is observed, being the difference with the maximum observed in the molar magnetic susceptibility of, approximately, 1%. This fact indicates the existence of a three-dimensional magnetic ordering around this temperature. The value of C_{mag} in the maximum is 22 J/kmol that corresponds to 7.3 J/kmol per paramagnetic Cu(II) and Ni(II) metallic cations.

3.3. Nuclear structure

The nuclear structure of $CuNi_2(PO_4)_2$ was refined using the Rietveld method to treat the room temperature D2B powder diffraction pattern ($\lambda = 1.594$ Å), taking as starting model the atomic coordinates of $CuNi_2(PO_4)_2$ synthesized by Goñi et al. [15]. The diffractogram at 100 K is shown in Fig. 4. The room temperature structural parameters and reliability factors from D2B data refinement are summarized in Table 1. The final refined positional and thermal parameters are given in Table 2. The interatomic bond distances and angles are included as supplementary material.

The crystal structure of $CuNi_2(PO_4)_2$ is shown in Fig. 5. The structure can be described as three-dimensional, being built by three different coner sharing polyhedra: PO_4 tetrahedra, MO_4 planar squares and square pyramidal M_2O_8 dimers. Each M_2O_8 dimer is linked to the adjacent dimers through the PO_4 groups. The MO_4 square planar entities do not present direct connection between them and are corner-sharing the M_2O_8 dimers. Attempts performed to refine the fraction of the Cu(II) and Ni(II) cations in order to deduce a possible disorder in the two sites confirmed that the MO_4 polyhera are totally occupied by the Cu(II) cations, whereas on the five-fold coordinated polyhedra are placed the Ni(II) cations. This latter coordination is unusual for this ion, and only a few number of compounds exhibiting this coordination have been found [22–24].

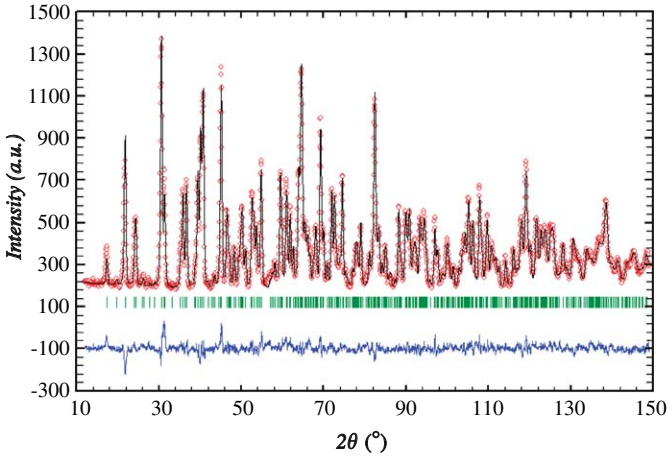

Fig. 4. Diffractogram at 100 K for $CuNi_2(PO_4)_2$.

Table 1
Details of Rietveld refinement from D2B neutron diffraction pattern at 100 and 2.0 K for $CuNi_2(PO_4)_2$

Temperature (K)	100	2.0
Molecular weight (g mol^{-1})	370.9	
Crystal system	Monoclinic	
Space group	$P2_1/n$ (No. 14)	
Angular range (deg)	10.0–150.0	10.0–140.0
a/Å	6.385(1)	6.383(1)
b/Å	9.292(1)	9.293(1)
c/Å	4.723(1)	4.721(1)
β/deg	90.66(1)	90.68(1)
V/Å^3	280.2(1)	280.0(1)
Reliability factors (%)		
$R_p = \Sigma\|yi_{obs} - (1/c)yi_{calc}\|/\Sigma yi_{obs}$	3.70	3.81
$R_{wp} = [\Sigma wi\|yi_{obs} - (1/c)yi_{calc}\|^2/\Sigma wi[yi_{obs}]^2]^{1/2}$	4.74	4.96
$R_B = \Sigma\|I_{obs} - I_{calc}\|/\Sigma I_{obs}$	4.61	4.78
Magnetic R-factor	—	13.8
χ^2	3.83	4.22

Table 2
Atomic coordinates and thermal parameters for $CuNi_2(PO_4)_2$ from D2B neutron diffraction data at 100 K

Atom	Wyckoff position	x	y	z	B (Å^2)
Cu	2a	0.5	0.5	0.5	0.17 (4)
Ni	4e	0.6538 (2)	0.1242 (1)	0.4749 (3)	0.73 (1)
P	4e	0.6546 (5)	0.3175 (3)	0.9930 (7)	0.59 (4)
O(1)	4e	0.3776 (4)	0.6754 (3)	0.6814 (5)	0.60 (4)
O(2)	4e	0.8437 (4)	0.4151 (2)	0.9243 (5)	0.49 (4)
O(3)	4e	0.6822 (4)	0.1634 (3)	0.9023 (5)	0.65 (4)
O(4)	4e	0.4607 (4)	0.3830 (3)	0.8446 (5)	0.81 (5)

The polyhedron of the Ni(II) ions in $CuNi_2(PO_4)_2$ shows bond distances ranging from 1.964(6) to 2.079(6) Å and O–Ni–O angles from 80.4°(4) to 170.4(5)°. The polyhedron distortion parameter, Δ, has been calculated using the model developed by Muetterties and Gugenberger [25]. The value, 84%, indicates a geometry near to the square-planar pyramid in which $\Delta = 1$. The coordination polyhedron of Cu(II) ions is square planar with a slight rhombic distortion. The Cu–O distances show two different values, 1.987(6) and 2.057(6) Å, and the O–Cu–O angles are slightly deflected from the ideal value of 90°.

3.4. Low-temperature neutron diffraction

The low-temperature pattern at 2.0 K exhibits extra magnetic peaks at 2θ, 19.37° and 24.87°, indicating that the compound is magnetically ordered (Fig. 6).

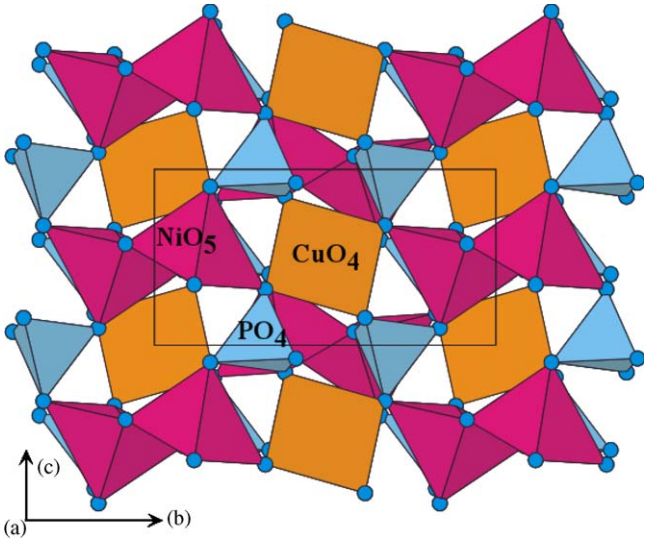

Fig. 5. Polyhedral representation of the crystal structure of $CuNi_2(PO_4)_2$.

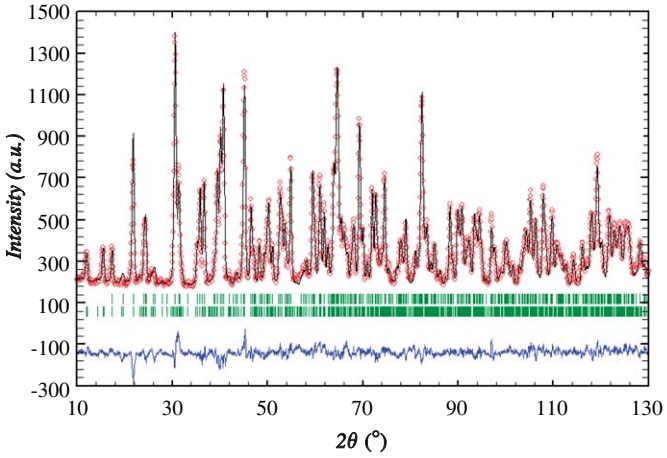

Fig. 6. Refinement of D2B neutron diffraction profile at 2.0 K ($\lambda = 1.594$ Å). The positions of the Bragg reflections for the nuclear (top) and magnetic (bottom) structures are presented. The different curves are plotted at the bottom of the figure with the same scale.

The magnetic peaks can only be indexed considering a magnetic lattice in which the "a" and "c" unit-cell parameters are duplicated with respect to those of the nuclear unit-cell, with a propagation vector of $[\frac{1}{2}, 0, \frac{1}{2}]$. The magnetic structure was analyzed using the macroscopic theory of Bertaut [26]. Taking into account that the Ni(II) ion is placed on a general position with multiplicity four, whereas that the Cu(II) ion is on a inversion center with multiplicity two, it is possible to generate all the atomic coordinates using the symmetry operations of the $P2_1/n$ space group, in which this phase crystallizes. The basis vectors corresponding to the different coupling of the magnetic moments in every sublattice are: for the Ni(II) sublattice $F = R1 + R2 + R3 + R4$, $G = R1 - R2 + R3 - R4$, $C = R1 + R2 - R3 - R4$, $A = R1 - R2 - R3 + R4$ and for the Cu(II) sublattice $F = S1 + S2$, $G = S1 - S2$. The possible

Table 3
Possible representations for the magnetic structure of $CuNi_2(PO_4)_2$

Modes Γ_n (2_1n)	Ni (R)			Cu (S)		
	x	y	z	x	y	z
Γ_1 (+ +)	C_x	F_y	C_z	G_x	F_y	G_z
Γ_2 (+ −)	G_x	A_y	G_z	—	—	—
Γ_3 (− +)	A_x	G_y	A_z	—	—	—
Γ_4 (− −)	F_x	C_y	F_z	F_x	G_y	F_z

representations for the magnetic structure of $CuNi_2(PO_4)_2$ are given in Table 3.

The Γ_1 and Γ_4 magnetic models indicate that both the sublattices of Ni and Cu ions are ordered, whereas that the Γ_2 and Γ_3 modes correspond to a behavior in which only the sublattice of the Ni(II) ion is ordered. All the Bertaut modes were studied, performing the profile analysis of the diffractograms carried out at 2.0 K. The fits were performed using the Rietveld method (FULLPROF program) [18]. The starting nuclear model was that obtained from the refinement carried out with the diffractograms collected at high temperature, considering simultaneously the nuclear and magnetic phases. The best fits between the experimental and theoretical diffractograms were obtained with the Bertaut mode Γ_4 that corresponds with the situation: Ni (R); $F(+++-)_x$, $C(++--)_y$, $F(+++-)_z$ and Cu (S); $F(+-)_x$, $G(+-)_y$, $F(+-)_z$. The components of the spins for every magnetic ion inside the nuclear unit-cell are $R1$: $M_x = 0.34(9)$, $M_y = 1.25(4)$, $M_z = 0.4(1)$; $R2$: $M_x = 0.34(9)$, $M_y = 1.25(4)$, $M_z = 0.4(1)$; $R3 = M_x = 0.34(9)$, $M_y = -1.25(4)$, $M_z = 0.4(1)$; $R4$: $M_x = 0.34(9)$, $M_y = -1.25(4)$, $M_z = 0.4(1)$ for the Ni(II) cation and $S1$: $S_x = 0.51(9)$, $S_y = -0.66(5)$, $S_z = 0.7(2)$; $S2$: $S_x = 0.51(9)$, $S_y = 0.66(5)$, $S_z = 0.7(2)$ for the Cu(II) ion. The total magnetic moments obtained for both Ni(II) and Cu(II) cations belonging to the crystal structure of this compound are $MR = 1.35(5)$ and $MS = 1.1(1)\,\mu_B$, respectively. The magnetic moment obtained for the Ni(II) cation is lower than that expected for an ion with spin $S = 1$. This reduction could be attributed to the five-fold coordination that exhibits this cation in the title compound. In our knowledge, the absence of bibliographic data concerning to this coordination it precludes to establish comparisons. In this magnetic structure, the Ni(II) ions displayed their magnetic moments predominantly along the y-axis, with small components in the x and z-axis. The Cu(II) cations, present a spatial disposition of their spins with similar components along the three axis.

The results indicate a magnetic structure in which the Ni(II) ions are ferromagnetically coupled inside the Ni_2O_8 dimers (R1−R2 and R3−R4) (Fig. 7). These dimers are antiferromagnetically coupled between them along the y-axis. The sublattice of Cu(II) ions exhibit antiferromagnetic couplings along the y-axis. According to this model, the components in the [100] and [001] do not cancel inside

the nuclear unit-cell. However, as the magnetic cell has a $[\frac{1}{2}, 0, \frac{1}{2}]$ propagation vector the "*a*" and "*c*" parameters of the magnetic unit-cell are duplicated along these directions with respect to the nuclear unit-cell. This fact originate a change of the sign in the orientation of the magnetic moments, cancelling the components M_x and M_z. So, this magnetic model is purely antiferromagnetic, in good agreement with the results obtained from the magnetic measurements.

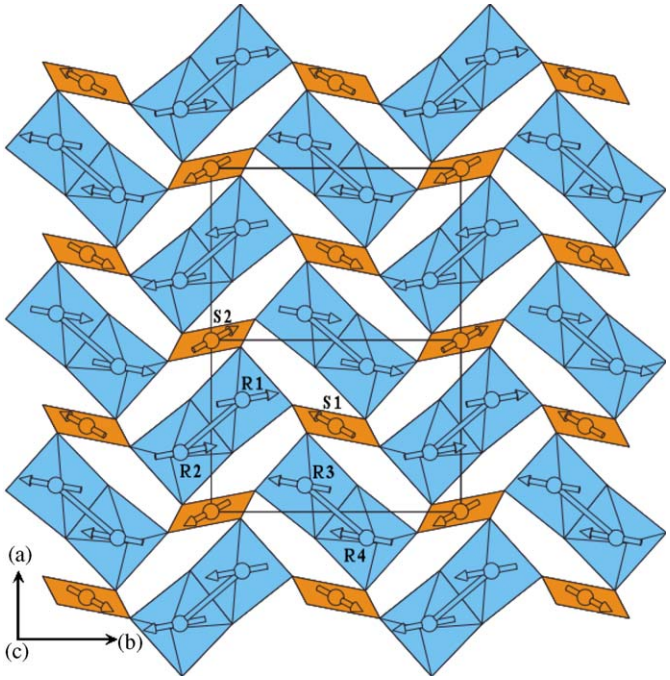

Fig. 7. Orientation of the the Ni [R] and Cu [S] moments in the magnetic structure of $CuNi_2(PO_4)_2$ along the "*ab*" plane.

3.5. Magnetostructural correlations

Considering the structural features of the $CuNi_2(PO_4)_2$ orthophosphate (see Fig. 8) two intermetallic exchange pathways can be proposed, in accordance with Goñi et al. [15], which are marked with arrows in Fig. 8.

The magnetic pathway through the (a) direction would run along the (101) plane through the Cu–O(4)–Ni–O(1)–Cu–heterometallic way. The intermetallic angles show values of 115° and 130°, respectively and, consequently the couplings would be antiferromagnetic. The interaction could take place between the two-half-filled orbitals $d_x2_{-y}2$ and d_z2 of Ni(II) and the homologous orbitals of the Cu(II) ion, which have only one unpaired electron. As the magnetic moment of the Ni(II) ion has theoretical twice the value of that corresponding to the Cu(II) ion, the interaction between these two metallic ions can give rise to the presence of uncompensated spins originating a ferromagnetic character in this exchange pathway. The magnetic system would be distributed in the plane (101) with alternating $S = \frac{1}{2}$, $S = 1$ spins and two alternating *J*-values, which are similar in sign but not in magnitude. Unfortunately, the presence of alternating *J*-values in the system together with the ignorance of the *g*-values for each magnetic cation makes the fit of the experimental curve difficult. The second exchange pathway (b) would take place inside the Ni_2O_8 dimers, in which the two Ni(II) ions interact through the two shared symmetrical O(2) oxygens. The value of the intermetallic angle of 99° does not allow the prediction of the type of the magnetic interactions present in this pathway [27]. The Ni–Ni distance inside the dimer presents a value of, approximately, 3.3 Å, and so, any contribution of direct exchange could not be considered in the magnetic structure of this phase. Finally, a

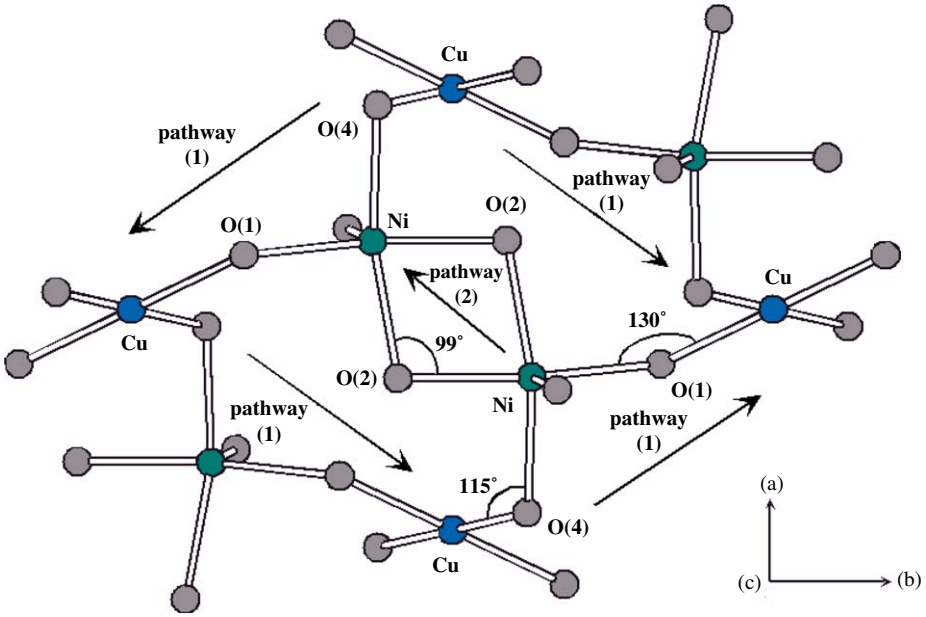

Fig. 8. Scheme of the magnetic exchange pathways in the *ab*-plane for $CuNi_2(PO_4)_2$.

third exchange pathway through the PO_4 groups could also be considered. This fact, similar to that observed in other phosphate compounds [28], gives rise to the three-dimensional character of this system. As a result, a total cancellation of the magnetic moments takes place establishing the global antiferromagnetic ordering in this system.

4. Concluding remarks

$CuNi_2(PO_4)_2$ exhibits three-dimensional antiferromagnetic couplings with a Neel temperature of 29.8 K. The specific heat data show a 3D magnetic ordering peak (λ-type) at 29.5 K, in good agreement with the magnetic data. The neutron diffraction pattern at 2.0 K exhibits extra magnetic peaks indicating that the compound is magnetically ordered at low temperatures. The magnetic structure is consistent with an antiferromagnetic phase with the presence of ferromagnetic couplings inside the Ni_2O_8 square pyramidal dimers.

Acknowledgments

This work was financially supported by the Ministerio de Educación y Ciencia (MAT 2004-02071) and Universidad del País Vasco/EHU (9/UPV00130.310-15967/2004; 9/UPV00169.310-13494/2001) and the "Fondo Europeo de Desarrollo Regional (FEDER), which we gratefully acknowledge. We thank Dr. M.T. Fernandez-Diaz from the ILL (Grenoble, France) for technical support for neutron measurements.

References

[1] R.C. Haushalter, L.A. Mundi, Chem. Mater. 4 (1992) 31.
[2] A. Clearfield, Chem. Rev. 88 (1988) 125.
[3] P.B. Moore, Am. Miner. 57 (1972) 24.
[4] L.W. Fingers, Am. Crystallogr. Assoc. Summer Meeting, Carleton University, Ottawa, Canada, 1970, p. 66.
[5] J.C. Joubert, G. Berthet, E.F. Bertaut, Z. Kristallogr. 136 (1972) 98.
[6] C. Calvo, R. Faggiani, Can. J. Chem. 53 (1975) 1516.
[7] G.L. Shoemaker, J.B. Anderson, E. Kostiner, Acta Crystallogr. B 33 (1977) 2969.
[8] J. Escobal, J.L. Pizarro, J.L. Mesa, J.M. Rojo, B. Bazan, M.I. Arriortua, T. Rojo, J. Solid State Chem. 178 (2005) 2626.
[9] J.B. Forsyth, C. Wilkinson, S. Paster, H. Effenberger, J. Phys.: Condens. Matter 2 (6) (1990) 1609.
[10] J.M. Rojo, J.L. Mesa, L. Lezama, T. Rojo, J. Mater. Chem. 7 (11) (1997) 2243.
[11] J.M. Rojo, J.L. Mesa, R. Calvo, L. Lezama, R. Olazcuaga, T. Rojo, J. Mater. Chem. 8 (6) (1998) 1423.
[12] J.L. Mesa, J.L. Pizarro, L. Lezama, J. Escobal, M.I. Arriortua, T. Rojo, J. Solid State Chem. 141 (1998) 508.
[13] J.M. Rojo, J.L. Mesa, L. Lezama, T. Rojo, J. Solid State Chem. 145 (1999) 629.
[14] J.L. Mesa, A. Goñi, L. Lezama, J.L. Pizarro, R. Olazcuaga, T. Rojo, Ann. Chim. Sci. Mater. (1999) S21.
[15] A. Goñi, L. Lezama, J.L. Pizarro, J. Escobal, M.I. Arriortua, T. Rojo, Chem. Mater. 11 (1999) 1752.
[16] J.L. Mesa, A. Goñi, A.L. Brandl, O. Moreno, G.E. Barberis, T. Rojo, J. Mater. Chem. 10 (2000) 2779.
[17] H.M. Rietveld, J. Appl. Crystallogr. 2 (1969) 65.
[18] J. Rodriguez-Carvajal, Physica B 192 (1993) 55.
[19] A.K. Cheetham, P. Day, Solid State Chemistry, Techniques, Oxford University Press, Oxford, 1991.
[20] P. Debye, Ann. Phys. 39 (1912) 789.
[21] J.M. Rojo, J.L. Mesa, L. Lezama, J.L. Pizarro, M.I. Arriortua, J. Rodríguez-Fernández, G.E. Barberis, T. Rojo, Phys. Rev. B 66 (2002) 94406.
[22] F. Basolo, R.G. Pearson, Mechamisms of Inorganic Reactions, Wiley, New York, 1967.
[23] K. Lukaszewicz, Bull. Acad. Pol. Sci. 47 (1967) 51.
[24] L. Galoisy, G. Calas, Mater. Res. Bull. 28 (1993) 221.
[25] E.L. Muetterties, L.J. Guggenberger, J. Am. Chem. Soc. 96 (1974) 1748.
[26] E.F. Bertaut, Acta Crystallogr. A 24 (1968) 217.
[27] J.B. Goodenough, Magnetism and the Chemical Bond, Interscience, New York, 1963.
[28] J.B. Forsyth, C. Wilkinson, S. Paster, B.M. Wanklyn, J. Phys. C.: Solid State Phys. 21 (1988) 2005.